Kinetic Analysis of the Divergence of Reaction Pathways in the Chiral *Lewis* Base Promoted Aldol Additions of Trichlorosilyl Enol Ethers: A Rapid-Injection NMR Study

by **Scott E. Denmark*** and **Son M. Pham**

Department of Chemistry, Roger Adams Laboratory, University of Illinois, 600 S. Mathews Avenue, Urbana, Illinois 61801, U.S.A. (e-mail: denmark@scs.uiuc.edu)

Dedicated with admiration and gratitude to Professor *Albert Eschenmoser* on the occasion of his 75th birthday

The aldol addition reaction of trichlorosilyl enol ethers and aldehydes with and without chiral *Lewis* base catalysts has been kinetically analyzed. The uncatalyzed reactions display classic first-order dependence on each component. The reactions catalyzed by bulky chiral phosphoramide **5** were examined by *ReactIR* and exhibited first-order dependence on the catalyst. To examine the kinetic behavior of the reaction catalyzed by phosphoramide **4**, a Rapid-Injection (RI) NMR apparatus was constructed and employed to allow rapid *in-situ* mixing and monitoring of the reaction course. The aldol addition catalyzed by **4** displayed second-order dependence on phosphoramide, thus providing direct evidence that two catalyzed pathways (with complimentary stereochemical consequences) exist that depend on phosphoramide structure and concentration. *Arrhenius* activation parameters for all three reactions showed striking characteristics of negligible enthalpies and extremely high entropies of activation. Comparison of these values was precluded by the existence of complex preequilibria in the catalyzed process.

1. Introduction. – Recent disclosures from these laboratories have illustrated the utility of chiral *Lewis* base catalysis in asymmetric aldol additions as demonstrated by the reaction of trichlorosilyl enol ether **1** with benzaldehyde in the presence of catalytic amounts of phosphoramides [1]. The addition provides aldol products in very high enantio- and diastereoselectivity with 10 mol-% phosphoramide (*S*,*S*)-**4** (*Scheme 1*).

Scheme 1

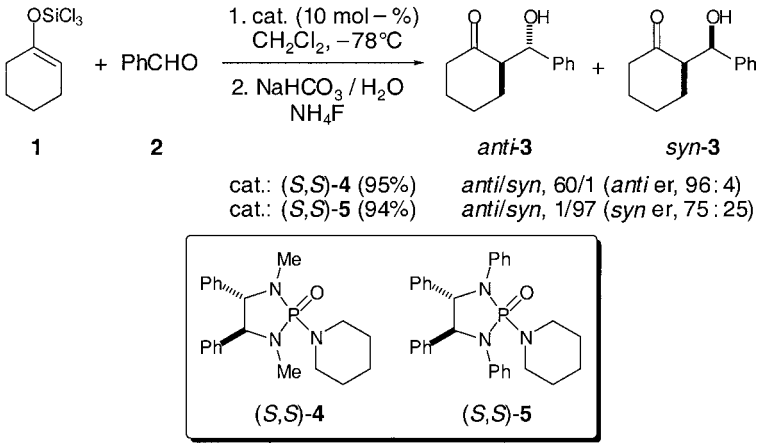

One of the most remarkable features of this process is the dramatic dependence of the *syn*/*anti* diastereoselectivity on the bulkiness and loading of the catalyst (*cf.* **4** *vs.* **5**) [1e]. To explain this behavior, we proposed that the reaction proceeds through independent pathways to the two diastereoisomers, which respond differently to catalyst size and concentration. Thus, we postulated a competition between one and two phosphoramide pathways, the former being operative at lower catalyst concentration (to the *syn*-isomer), while the latter is operative at higher catalyst concentrations (to the *anti*-isomer) (*Scheme 2*).

Scheme 2. *Divergent Mechanistic and Stereochemical Pathways*

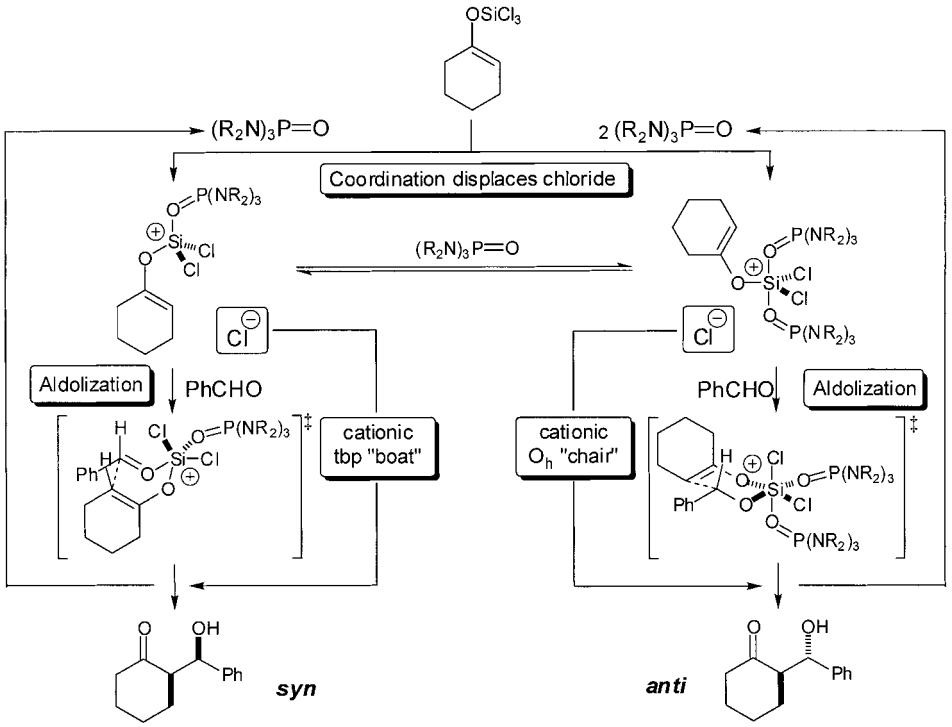

In support of this hypothesis, we demonstrated that catalyst **4** exhibits a positive nonlinear effect, fitting well with *Kagan*'s two-ligand model [2]. Furthermore, the more hindered catalyst **5** shows linear asymmetric induction, providing indirect evidence that a single phosphoramide is present in the configuration-determining step. The effects of added salts (common ion effect) lent credence to the premise of chloride ionization to provide cationic siliconate intermediates to accommodate all the ligands [1e]. We now report *direct* kinetic evidence that confirms the existence of dual pathways and additional insights that clarify the origin of rate enhancement.

2. Results and Discussion. – For the initial kinetics studies, we examined the uncatalyzed reaction between trichloro[(1-methylethenyl)oxy]silane (**6**) [1d] to

pivalaldehyde (**7**), as shown in *Scheme 3*[1]). The overall reaction order could be determined for the uncatalyzed reaction by employing pseudo-order conditions. With 10 equiv. of **7**, the reaction was determined to be first-order ($R^2 = 0.9999$) in **6** by virtue of a best-fit analysis of first- and second-order functions[2]). Likewise, with 10 equiv. of **6**, the reaction was determined to be first-order in **7**. Thus, the uncatalyzed aldol addition was determined to be second-order overall, giving the classical bimolecular rate expression of d[product]/dt = k[enolate][aldehyde].

Scheme 3

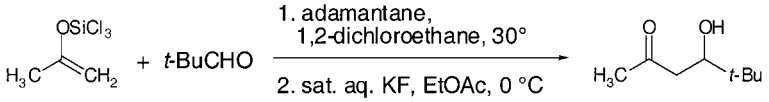

6 **7** **8**

Arrhenius activation parameters were then determined over a temperature range from 25 to 60° (*Table 1*)[3]). The major contribution to the free energy of activation ($\Delta G^{\ddagger}$) is the entropy of activation ($\Delta S^{\ddagger}$). Such a large negative $\Delta S^{\ddagger}$ is indicative of a highly organized transition structure or a highly unfavorable preequilibrium (for additional examples of kinetic studies on aldol additions, see [3a,b]; for an *ab initio* MO study, see [3c]). The $\Delta H^{\ddagger}$ is surprisingly small and suggests a high level of activation in the binary complex[4]).

Whereas classic kinetic studies from reaction quenching were suitable for the uncatalyzed reactions, the rate of aldolization in the presence of phosphoramide was far too great for this technique. Towards this end, the kinetic parameters of the aldolization were determined by *in-situ* monitoring by the use of a *ReactIR 1000* instrument[5]). To vouchsafe the results from this method, the activation parameters of the uncatalyzed process were determined for comparison. Changes in the absorbance of the enolic C=C bond, as well as the C=O group of the aldehyde, corresponding to internal changes in concentration for the given species, could easily be recorded as a function of time. Data from the *ReactIR* were in excellent agreement with the values obtained through GC analysis (*Table 1*)[6]). Another benefit of *in-situ* monitoring with *ReactIR* is the ability to use aromatic aldehydes **2** and substituted enolates **1** as *syn*- and *anti*-aldolates are indistinguishable and do not suffer *retro*-aldolization. The results of the uncatalyzed

---

[1]) Our decision to use a methyl ketone enolate obviated the need to analyze mixtures of diastereoisomers, greatly simplifying the kinetic analysis. All attempts to study the addition of **6** to **2** resulted in *retro*-aldolization during GC analysis. In fact, aldol products of all aromatic aldehydes gave similar results by GC analysis.

[2]) All raw kinetic data and plots of *Arrhenius* functions are available upon request.

[3]) Entries at each temperature were determined in triplicate to give a high correlation factor for the *Arrhenius* plot.

[4]) We assume that the rate-determining step in the uncatalyzed reaction is the aldol addition, and that complexation of the aldehyde is reversible.

[5]) *ReactIR*™ *1000* fitted with a 5/8″ *DiComp*™ Probe, running software Version 2.1a. *ASI Applied Systems, Inc.*, 8223 Cloverleaf Drive, Suite 120, Millersville, MD 21108, U.S.A.

[6]) Comparing the activation parameters determined by each analytical method shows that GC analysis provided a remarkably high level of precision as compared to *ReactIR* analysis. This is understandable when considering the sensitivity of flame-ionization detectors fitted on modern GC spectrometers.

reaction between **1** and **2** were in line with the previous example (*Table 1*). The activation parameters reflect the considerably faster rate of this combination.

Table 1. Arrhenius *Activation Energies for Aldol Additions of Trichlorosilyl Enolates*[a])

Conditions	Method	E*a* [kcal mol^{-1}]	*A* [M^{-1} s^{-1}]	$\Delta H^{\neq}$ [kcal mol^{-1}]	$\Delta S^{\neq}$ [cal mol^{-1} K^{-1}]	$\Delta G^{\neq}$ [kcal mol^{-1}]
Uncatalyzed **6**+**7**	GC	6.4 ± 0.002	865 ± 7	5.8 ± 0.1	− 56.7 ± 0.1	23.0 ± < 0.1
Uncatalyzed **6**+**7**	*ReactIR*	6.5 ± 0.1	936 ± 117	5.9 ± 0.1	− 55.4 ± 0.2	22.6 ± 0.2
Uncatalyzed **1**+**2**	*ReactIR*	3.0 ± 0.5	314 ± 258	2.4 ± 0.5	− 58.2 ± 1.6	20.0 ± 1.0
1+**2**, 5 mol-% **5**	*ReactIR*	0.9 ± 0.1	5.1 ± 1.7	0.3 ± 0.1	− 67.1 ± 0.7	20.6 ± 0.2
1+**2**, 5 mol-% **5**	RINMR	1.8	0.4	1.2	− 63.3	20.4
1+**2**, 10 mol-% **4**	RINMR	2.1 ± 0.5	224 ± 100	1.5 ± 0.5	− 51.9 ± 1.0	17.3 ± 1.0

[a]) Activation parameters were calculated for $T = 303$ K.

The catalyzed aldol additions between **1** and **2** were first examined in the presence of phosphoramide **5**. The reaction displayed first-order dependence on **5** ($R^2 = 1.0000$), over typical catalyst loadings at $-35°$[2]). This provided direct evidence for the presence of a single catalyst molecule in the transition state when a bulky phosphoramide is employed. Extrapolation to 0 mol-% catalyst gave an unrealistically high value for the theoretical background reaction, which prompted us to examine the reaction rates at much lower catalyst concentrations (*Fig. 1*). The sharp change in slope at low catalyst loadings is consistent with a change in mechanism, thus supporting our hypothesis that the catalyzed pathway involves cationic silicon intermediates.

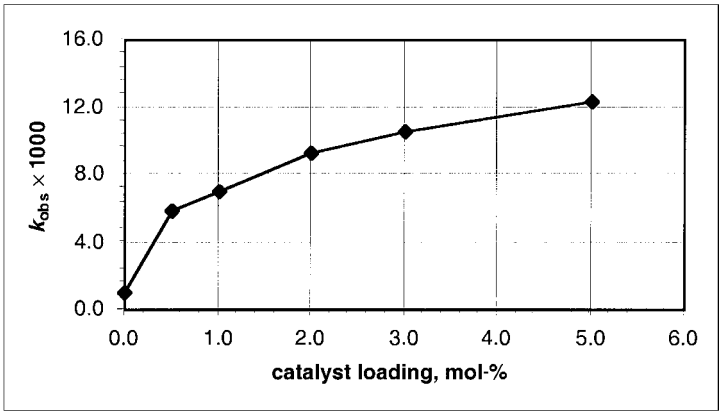

Fig. 1. *Plot of* k_{obs} *vs. catalyst loading for the addition of* **1** *to* **2** *catalyzed by* **5**

Activation parameters for the catalyzed reaction could be determined as before, now over a temperature range of -11 to $-65°$. As was seen for the addition of **6** to **7**, $\Delta G^{\neq}$ for the catalyzed reaction is dominated by the contribution from $\Delta S^{\neq}$ and even less dependent on $\Delta H^{\neq}$. The nearly vanishing $\Delta H^{\neq}$ again hints at still greater activation in the ternary complex. As expected, $\Delta S^{\neq}$ is greater for the catalyzed compared to the uncatalyzed addition, because the entropic demands for the ternary complex are expected to be substantially greater than for a binary complex. Comparison of

activation free energies shows a surprising similarity between the uncatalyzed and catalyzed reactions. However, in the catalyzed reaction, there is a rapid preequilibrium complexation of enolate and phosphoramide[7]). Since it has not been possible to determine the magnitude of these preequilibria[8]), we are unable to extract the parameters to allow comparison with the uncatalyzed reaction[9]).

Three limiting scenarios for K_{eq} can be envisioned to probe the consequences on the activation parameters (*Table 2*). Varying the magnitude of K_{eq} does not effect the value for $\Delta H^{\ddagger}$, but will alter the value for $\Delta S^{\ddagger}$ and consequently $\Delta G^{\ddagger}$. The trend apparent in *Table 2* is that, even at very low concentrations of reactive complexes, $\Delta S^{\ddagger}$ is still highly negative, suggestive of a high degree of order in the aldolization transition structure or a highly unfavorable aldehyde binding equilibrium.

Table 2. *Effect of Preequilibrium Complexation Constant on Activation Parameters*[a])

Catalyst	Parameter [unit]	No preequilibrium	$K_{eq} > 100$	$K_{eq} = 0.11$	$K_{eq} = 0.01$
5	$\Delta S^{\ddagger}$ [eu]	−67.1	−56.9	−53.6	−48.9
5	$\Delta G^{\ddagger}$ [kcal mol^{-1}]	20.6	17.6	16.5	15.1
4	$\Delta S^{\ddagger}$ [eu]	−51.9	−41.2	−36.8	−32.2
4	$\Delta G^{\ddagger}$ [kcal mol^{-1}]	17.3	14.0	13.1	11.6

[a]) Activation parameters were calculated for $T = 303$ K.

Kinetics studies of addition of **1** to **2** catalyzed by phosphoramide **4** using the *ReactIR* were inconclusive. Extremely fast reaction rates, limited instrument sensitivity, and a low-temperature operating limit of −80° conspired to thwart these efforts. To address these limitations (and provide a general solution to problems presented by fast reactions), we have designed and built a Rapid-Injection NMR (RINMR) apparatus[10]). The availability of highly sensitive NMR probes with temperature ranges from −150 to +150° make NMR spectroscopy a superior analytical tool for both the determination of kinetic profiles, as well as structure determination of reactive intermediates[11]).

To establish that RINMR could provide accurate kinetic measurements, we reexamined the addition of **1** to **2** catalyzed by **5** to provide a calibration of the newly built apparatus. *Arrhenius* parameters were determined by the injection of a solution of **2** into an open, spinning NMR tube containing both **1** and **5** under an atmosphere of N_2 at low temperatures. Gratifyingly, RINMR analysis provided good agreement with the previous *ReactIR* studies (*Table 1*). Thus secured, we undertook the more challenging

7) Additional preequilibria for dissociation of chloride and reversible binding of aldehyde are also likely contributors.

8) Low-temperature NMR analysis of chlorosilyl enol ethers and phosphoramides show dynamic behavior down to −120°; X. Su, Ph.D. Thesis, University of Illinois, 1998.

9) The possibility that binding aldehyde has become rate-determining in the catalyzed reactions cannot be excluded.

10) For examples of the use of rapid injection NMR techniques, see [4].

11) The design, construction, and implementation of the RINMR apparatus will be the subject of forthcoming disclosures. Inquires are encouraged.

study of catalyzed reactions using **4**. ^{1}H-NMR Analysis permitted operation at lower concentrations than previously possible for the reaction of **1** and **2**. A log plot of the rate constant (k_{obs}) *vs.* catalyst concentration allowed for the determination that aldol addition has a second-order dependence ($m = 2.113$) on **4** (*Fig. 2*)[2]). This provided direct evidence for the existence of a mechanistic dichotomy between catalyst **4** and **5**, namely that reactions using **4** proceed through a two-phosphoramide pathway, whereas reactions using **5** proceed through a one-phosphoramide pathway. Additionally, a two-phosphoramide mechanism provides unambiguous substantiation of the origin of nonlinear asymmetric induction observed for **4**.

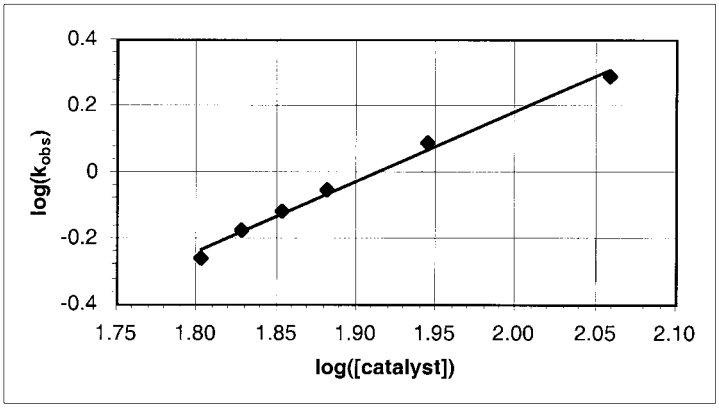

Fig. 2. *Plot of log* (k_{obs}) vs. *log ([catalyst]) for the addition of* **1** *to PhCHO catalyzed by* **4** *at* $T = -80°$. The graph depicts the linear fit to $f(x) = mx + b$ ($m = 2.113$, $R^2 = 0.992$).

Activation energies were then determined using 10 mol-% catalyst between -70 and $-90°$[12]). A comparison of the *Arrhenius* activation parameters for the two different catalysts shows a substantial decrease in $\Delta G^{\ddagger}$ for the aldol addition using **4** (*Table 1*). Specifically, the decrease in $\Delta G^{\ddagger}$ is a result of a more favorable $\Delta S^{\ddagger}$ as there is little change in $\Delta H^{\ddagger}$. In keeping with the foregoing discussion, we are unable to assess the contributions of the various activation parameters because of the existence of multiple complexation preequilibria of unknown magnitude. Again, assuming limiting values for K_{eq} we see the same trend (*Table 2*), albeit with consistently reduced $\Delta S^{\ddagger}$ contributions compared to the reactions with **5**. Although the existence of complex preequilibria preclude comparison among the three types of reactions, it is still worth noting that each of these transformations is characterized by an extremely low $\Delta H^{\ddagger}$ and strikingly high $\Delta S^{\ddagger}$ both characteristics of enzymatic catalysis. We are currently attempting to establish the rate-determining step and to assay the magnitude of the preequilibria by indirect methods.

---

[12]) Attempts to extend this temperature domain while maintaining CD_2Cl_2 as the bulk solvent proved unsuccessful due to extremely fast reaction rates for temperatures above $-65°$. Consequently, decreasing the temperature to below $-90°$ results in highly viscous solutions and presents the possible risk of sample freezing.

3. Conclusions. – Aldol additions catalyzed by **5** proceed *via* a one-phosphoramide pathway, while those catalyzed by **4** proceed *via* a two-phosphoramide pathway. This dichotomy explains the dramatic catalyst-loading effect on diastereoselectivity, as well as the origin of the nonlinear asymmetric induction observed for phosphoramide **4**. Both catalyzed pathways most likely involved the ionization of chloride to afford cationic silicon intermediates greatly enhancing the relative rates of both reactions when compared to the uncatalyzed pathway.

We are grateful to the *National Science Foundation* for generous financial support (CHE 9803124). *S. M. P.* thanks the University of Illinois and the *Eastman Kodak Company* for Graduate Fellowships. We owe particular thanks to Mr. *Bruce Williams* for his help in the design and construction of the RINMR apparatus. The NMR spectrometers used in this study are part of the *Varian Associates*/*Oxford Instruments* Center for Excellence in Nuclear Magnetic Resonance.

Experimental Part

General. ^{1}H-NMR Spectra for all kinetic runs were recorded at the University of Illinois in the *Varian Oxford Instruments* Center for Excellence in NMR Laboratory using a wide bore *Varian Unity Inova* (500 MHz ^{1}H) spectrometer containing a 5-mm $^{15}N-^{31}P$ broad-band probe, in CD_2Cl_2 unless otherwise stated. Tredicator temps. were calibrated using standard methods involving ethylene glycol and MeOH as needed. Anal. GC was performed on a *Hewlett-Packard 5890* gas chromatograph equipped with a flame-ionization detector and a *Hewlett-Packard HP-5* (50 m) column or a *Hewlett-Packard Ultra-2* (50 m) column. The injector temp. was 225° (set to 160° for all kinetic experiments). The detector temp. was 300° with a split ratio of *ca.* 100 : 1. *Fourier*-transform IR analysis was performed using a *ReactIR 1000* purchased from *ASI Applied Systems*, *Inc.*, 8223 Cloverleaf Drive, Suite 120, Millersville, MD 21108, U.S.A. Reactions were monitored using a 5/8″ *DiComp* probe fitted to an MCT detector. Acquisitions were recorded using software Version 2.1a. All reactions were performed using oven (160°) and/or flame-dried glassware under an atmosphere of dry N_2, unless otherwise stated. Solvents and commercial reagents were purified using established procedures prior to use, with the exception of CD_2Cl_2, which was used directly from the ampoule.

2. *GC Kinetics Using Zeroeth-Order Aldehyde. General Procedure 1* (*GP 1*). *2,2-Dimethylpropanal* (*pivalaldehyde*; **7**; 1.16 ml), 10.4 mmol, 10 equiv.) was added rapidly to a soln. of trichloro[(1-methylethenyl)-oxy]silane (**6**; 150 µl, 1.04 mmol) and adamantane (22.3 mg, 0.16 mmol) in 1,2-dichloroethane (8 ml) at r.t. Small aliquots were removed *via* cannula directly into a cold (0°) soln. of conc. KF and 1.0M phosphate buffer (1 : 1, *v*/*v*). The mixture was vigorously vortexed and then was extracted with AcOEt. The mixture was passed through *Florisil* (plug) and quickly eluted with AcOEt. The sample was then analyzed by GC. Kinetic runs were performed between 20 and 65°.

3. *GC Kinetics Using Zeroeth Order Enol Ether. General Procedure 2* (*GP 2*). Pivalaldehyde (**7**; 29 µl, 0.26 mmol) was added rapidly to a soln. of **6** (380 µl, 2.6 mmol, 10 equiv.) and adamantane (6.8 mg, 0.05 mmol) in CH_2Cl_2 (2 ml) at r.t. Small aliquots were removed *via* cannula directly into a cold (0°) soln. of conc. KF and 1.0M phosphate buffer (1 : 1, *v*/*v*). The mixture was vigorously vortexed and then was extracted with AcOEt. The mixture was passed through *Florisil* (plug) and quickly eluted with AcOEt. The sample was then analyzed by GC. Kinetic runs were performed between 20 and 65°.

4. *Uncatalyzed* ReactIR *Kinetics. General Procedure 3* (*GP 3*). A dry reaction vessel was assembled onto the IR probe and was vented for several min. with dry N_2. 1,2-dichloroethane (1.5 ml) was then added to the reaction vessel, and a *background* file was collected. Enolate **1** (82 µl, 0.45 mmol) was then added and allowed to fully mix, and the soln. was left to equilibrate before beginning data collection. PhCHO (46 µl, 0.45 mmol) was added quickly to the enolate soln. IR Spectra were collected at 3 min intervals for 180 min at 30° by internal monitoring: recorded disappearance of peak at 1679 cm^{-1} (enolate C=C). Kinetic runs were performed between 30 and 60°.

5. *Phosphoramide-Catalyzed* ReactIR *Kinetics. General Procedure 4* (*GP 4*). Compound (±)-**5** (15 mg) was added to a dry reaction vessel. The vessel was assembled onto the IR probe and was vented for several min with dry N_2. Dry CH_2Cl_2 (2.3 ml) was then added to the reaction vessel. The vessel was then submerged in a chilled i-PrOH bath, and the contents were allowed to equilibrate prior to collecting a *background* file. Enolate **1** (111 µl, 0.61 mmol) was then added and allowed to fully mix. PhCHO (62 µl, 0.61 mmol) was added quickly to the reaction soln. IR Spectra were collected at 30-s intervals for 240 min at −49° by internal monitoring:

recorded disappearance of peak at 1679 cm^{-1} (enolate C=C). Kinetic runs were performed between −49 and −10°.

6. *Rapid-Injection NMR Kinetics Using Phosphoramide* **5**. *General Procedure 5* (*GP 5*). To a dry NMR tube was added phosphoramide **5** (8.6 mg, 0.017 mmol), CD_2Cl_2 (600 µl), and enolate **1** (65 ml, 0.35 mmol). The tube was vigorously mixed using a vortex shaker and was stored in a short *Dewar* flask at −78°. Following proper positioning in the spinner, the cap was carefully removed, and the tube was quickly lowered into a precooled spectrometer under dry N_2. The fully primed injection apparatus was then carefully lowered into the spinning tube, and the entire setup was allowed to equilibrate for several min. After equilibration, a PhCHO soln. (85 µl, 0.35 mmol) was then rapidly injected. Kinetic runs were performed between −58 and −27°.

7. *Rapid-Injection NMR Kinetics Using Phosphoramide* **4**. *General Procedure 6* (*GP 6*). To a dry NMR tube were added 3.2 mg (0.009 mmol) of phosphoramide **4**, 600 µl of CD_2Cl_2, 50 µl of a stock soln. of 1% TMS in $CDCl_3$, followed by 16 µl (0.086 mmol) of enolate. The tube was vigorously mixed using a vortex shaker and was stored in a short *Dewar* flask at −78°. Following proper positioning into spinner, the cap was carefully removed, and the tube was quickly lowered into a precooled spectrometer under dry N_2. The fully primed RINMR injection apparatus was then carefully lowered into the spinning tube, and the entire setup was allowed to equilibrate for several min. After equilibration a PhCHO soln. (42 µl, 0.086 mmol) was then rapidly injected. Kinetic runs were performed between −96 and −70°.

REFERENCES

[1] a) S. E. Denmark, S. B. D. Winter, X. Su, K.-T. Wong, *J. Am. Chem. Soc.* **1996**, *118*, 7404; b) S. E. Denmark, K.-T. Wong, R. A. Stavenger, *J. Am. Chem. Soc.* **1997**, *119*, 2333; c) S. E. Denmark, R. A. Stavenger, K.-T. Wong, *J. Org. Chem.* **1998**, *63*, 918; d) S. E. Denmark, R. A. Stavenger, S. B. W. Winter, K.-T. Wong, P. A. Barsanti, *J. Org. Chem.* **1998**, *63*, 9517; e) S. E. Denmark, X. Su, Y. Nishigaichi, *J. Am. Chem. Soc.* **1998**, *120*, 12990; f) S. E. Denmark, R. A. Stavenger, K.-T. Wong, X. Su, *J. Am. Chem. Soc.* **1999**, *121*, 4982; g) S. E. Denmark, R. A. Stavenger, *Acc. Chem. Res.* **2000**, *33*, 132.

[2] a) D. Guillaneux, S.-H. Zhao, O. Samuel, D. Rainford, H. B. Kagan, *J. Am. Chem. Soc.* **1994**, *116*, 9430; b) D. R. Fenwich, H. B. Kagan, *Top. Stereochem.* **1999**, *22*, 257; c) C. Girard, H. B. Kagan, *Angew. Chem., Int. Ed.* **1998**, *22*, 2922; d) M. Avalos, R. Babiano, P. Cintas, J. L. Jimenez, J. C. Palacios, *Tetrahedron: Asymmetry* **1997**, *8*, 2997.

[3] a) A. G. Myers, K. L. Widdowson, *J. Am. Chem. Soc.* **1990**, *112*, 9672; b) A. G. Myers, K. L. Widdowson, P. J. Kukkola, *J. Am. Chem. Soc.* **1992**, *114*, 2765; c) B. W. Gung, Z. Zhu, R. A. Fouch, *J. Org. Chem.* **1995**, *60*, 2860.

[4] a) J. F. McGarrity, J. Prodolliet, T. Smyth, *Org. Magn. Reson.* **1981**, *17*, 59; b) C. A. Palmer, C. A. Ogle, E. M. Arnett, *J. Am. Chem. Soc.* **1992**, *114*, 5619; c) M. T. Reetz, B. Raguse, C. F. Marth, H. M. Hügel, T. Bach, D. N. A. Fox, *Tetrahedron* **1992**, *48*, 5731.

Received May 3, 2000